

# Comment on hardness definitions

J. Malzbender

*Forschungszentrum Jülich GmbH, Institute for Materials and Processes in Energy Systems, 52425 Jülich, Germany*

Received 27 April 2002; received in revised form 5 September 2002; accepted 16 September 2002

## Abstract

The different definitions of hardness and elastic modulus as obtained using indentation with conical (also Vickers and Berkovich) or spherical indenters are compared and relationships that permit a conversion and an assessment of the differences are derived. A comparison to experimental data is given.

© 2002 Elsevier Science Ltd. All rights reserved.

*Keywords:* Hardness; Mechanical properties; Plasticity

## 1. Introduction

Indentation testing is widely used to assess the mechanical properties of materials, such as the elastic modulus and the hardness.<sup>1,2</sup> There is a wide choice of indenter geometries and materials, however, spherical indenters are used less frequently than pyramidal indenters,<sup>1–3</sup> since sharp indenters cause yielding of the indented material at a lower load and thus also permit to assess the properties of very thin films.<sup>4,5</sup> However, there are different definitions of hardness.

The effects of porosity on the hardness and grain structures have been analyzed in the literature.<sup>6</sup> In order to determine the mechanical properties of a material the analyzed volume should have a contact radius being approximately one order of magnitude larger than the characteristic length scale (pore or grain size).<sup>7,8</sup> Smaller ratios of diameter to characteristic length can lead to indentation size effects. Recently a experimental comparison has been made of the hardness obtained for ceramics on the basis of different definitions.<sup>9,10</sup> In this paper an attempt is made to derive equations that permit a conversion of hardness values determined under load and after load removal on the basis of different standards and definitions.

## 2. Theory and comparison

An example of a load-displacement curve obtained using indentation is shown in Fig. 1. For sharp indenters the Martens Hardness  $HM$ , also sometimes referred to hardness under test force (HVL), universal hardness  $HU^2$  or unreduced hardness,<sup>11</sup> can be defined as:<sup>12–14</sup>

$$HM = P/A \quad (1)$$

where  $A$  is the contact area of the indenter under load, which is  $A = \alpha h^2$  for sharp indenters, with  $h$  being the maximum depth under the load  $P$  (see Fig. 1). For a Vickers or Berkovich indenter  $\alpha = 26.43$  and  $26.44$ , respectively.<sup>2</sup> Generally, for a conical indenter the constant  $\alpha = \pi \tan \gamma \sqrt{1 + (\tan \gamma)^2}$ , where  $\gamma$  is the half-angle of the cone. For a spherical indenter  $A = (2\pi Rh)$ . It is important to note that this hardness definition incorporates elastic and plastic deformation.

A plastic hardness has been defined as:<sup>12–14</sup>

$$H_{pl} = P/A_r \quad (2)$$

where the plastically deformed area  $A_r$  is defined for sharp indenters as  $A_r = \alpha h_r^2$  and for spherical indenters as  $A_r = 2\pi R h_r$ , with  $h_r$  being the intersection with the abscissa of the tangent of the unloading curve at maximum load (see Fig. 1) which is:<sup>12,13</sup>

$$h_r = h_{max} - P/(dP/dh) \quad (3)$$

The more commonly used indentation hardness also sometimes referred to as reduced hardness<sup>11</sup> is given for these indenters as:<sup>3</sup>

\* Corresponding author.

E-mail address: [j.malzbender@fz-juelich.de](mailto:j.malzbender@fz-juelich.de) (J. Malzbender).

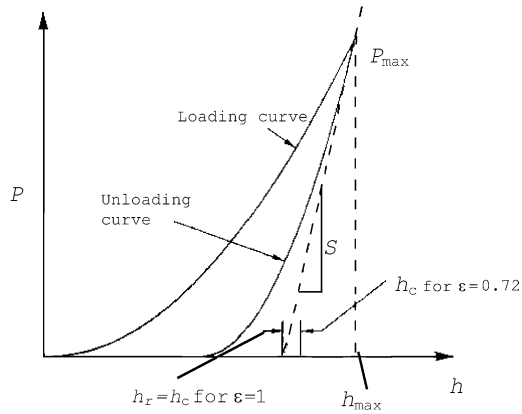


Fig. 1. Example of a load-displacement curve.

$$H = P/A_c. \quad (4)$$

where the contact area  $A_c$  for sharp indenters is  $A_c = (\sqrt{\pi} \tan \gamma h_c)^2$  and for spherical indenters  $A_c = 2\pi R h_c$  with  $h_c$  being the contact depth, i.e. the vertical distance along which contact is made (see Fig. 1), which is:<sup>3</sup>

$$h_c = h_{\max} - \varepsilon P / (dP/dh) \quad (5)$$

In fact, as explained below  $h_r$  is a special case of  $h_c$  generally valid only for a flat punch. Eq. (4) can be used for Berkovich and Vickers indenters via utilizing the concept of an equivalent conical indenter. For an ideal Vickers or Berkovich indenter this leads to  $\gamma = 70.3^\circ$ . The parameter  $\varepsilon$  is a geometric constant. It can be derived that it takes a value of 1 for a flat punch, 0.72 for conical and  $\varepsilon = 0.75$  for paraboloid indenters.<sup>3</sup> Often the Vickers Hardness  $H_V$  is used as a measure of plastic deformation, which is defined as:

$$H_V = \frac{2P \sin \phi}{d^2} \quad (6)$$

where  $d$  is the diagonal of the square impression and  $\phi$  is the half angle between the opposite faces of the pyramid. Since the projected area is  $d^2/2$ , the effective radius of the impression is  $a = (d^2/2\pi)^{1/2}$  and the mean indentation pressure is  $H = H_V / \sin \phi$ . Furthermore, sometimes  $H_V$  is still given as a hardness number and requires transfer into the SI unit Pa.

The effect of friction will lead to a change of the stress only for sharp indenters, i.e. cube corner indenters.<sup>15</sup> For typically used Spherical, Vickers or Berkovich indenters the effect of friction can be neglected for the case of plastic deformation, although for a sphere the position of the initiation of yield will be moved closer to the surface.<sup>16</sup>

Sakai<sup>17</sup> recently introduced a model to incorporate a “true hardness” which is independent of the indenter angle. Introducing a first order approximation of the expanding cavity model into the above equations would yield relationships depending only on the yield strength and thus also being independent of the indenter angle.

Eq. (4) is based on the projected area of the indentation and it was observed that the determined values agreed well with hardness measurements based on an optical measurement of the contact area after unloading, i.e. the Meyer Hardness.<sup>3</sup> Note that  $h_r$  is a special case of  $h_c$  for  $\varepsilon = 1$  and:

$$h_r/h_c = (1 - 1/\varepsilon)h/h_c + 1/\varepsilon \quad (7)$$

The use of  $\varepsilon = 1$  for  $h_r$  is based on calibration for metallic materials, whereas for ceramic materials different values have been suggested.<sup>18</sup> This difference is widely ignored in literature.<sup>12,19,20</sup> It can be suggested that the factor  $\varepsilon = 1$  might be an effect of pile-up during the measurements.<sup>3</sup> As will be shown later the difference between  $h_r$  and  $h_c$  is significant for some materials and can therefore lead to calibration errors. In fact, all hardness definitions given above have to be corrected for the effect of the hardening and related pile-up and sink-in of the material via the function  $f(n)$ .<sup>21</sup>

From Eqs. (1)–(4) the following relationships can be derived for conical indenters:

$$HM/H_{pl} = (h_r/h)^2 \quad (8)$$

and

$$HM/H = \pi/\alpha(\tan \gamma h_c/h)^2 \quad (9)$$

For spherical indenters the two hardness ratios become:

$$HM/H_{pl} = h_r/h \quad (10)$$

and

$$HM/H = h_c/h \quad (11)$$

Eqs. (8) and (9) permit a hardness conversion provided that the relevant depths are known. Furthermore, combination of Eqs. (7)–(9) yields for conical indenters:

$$H = \frac{\alpha/\pi(\tan \gamma)^2}{\left(\frac{1-\varepsilon}{\sqrt{HM}} + \frac{\varepsilon}{\sqrt{H_{pl}}}\right)^2} \quad (12)$$

and from Eqs. (7), (10) and (11) an equivalent relationship is obtained for spherical indenters:

$$H = HM / (1 - \varepsilon + \varepsilon HM/H_{pl}) \quad (13)$$

Simple mathematical transformation of Eq. (8) permits a determination of  $HM$  or  $H_{pl}$ . A general relation-

ship between  $h$  and  $h_c$  has been derived previously for conical indenters:<sup>21</sup>

$$h = \frac{h_c}{f(n)} \left[ 1 + \frac{\pi \tan \gamma}{2} \frac{\varepsilon H}{\beta E_r} \right] \quad (14)$$

and spherical indenters:<sup>21</sup>

$$h = h_c \left[ 1 + \frac{\pi \sqrt{R}}{\sqrt{2} f(n) h_c} \frac{\varepsilon H}{\beta E_r} \right] = \frac{\varepsilon \sqrt{HP\pi}}{2\beta E_r} + \frac{P}{2HRf(n)\pi} \quad (15)$$

Note that it has been shown that similar relationships to Eqs. (14) and (15) can be useful in the modeling of impact to predict when the kinetic energy transferred to the target becomes significant.<sup>22</sup>

$E_r$  is the reduced elastic modulus, which is commonly defined as:

$$\frac{1}{E_r} = \frac{1 - \nu_i^2}{E_i} + \frac{1 - \nu^2}{E} \quad (16)$$

where  $E_i$  and  $\nu_i$  are Young's modulus and Poisson's ratio of the indenter and  $E$  and  $\nu$  of the indented material, respectively. In the case of elastic deformation,  $H$  in Eq. (9) has to be substituted by the indentation pressure  $\sigma_H$ . The correction factor  $\beta$  is due to the fact that the boundary conditions used to derive elastic contact models employed in indentation allow for inward displacement of the surface.<sup>23</sup>

In the literature values of  $(E_r/Y) \approx 3 \tan \gamma$  and  $\approx 40 \tan \gamma$  for the onset of yield and fully plastic deformation under conical indenters, respectively, are suggested.<sup>24</sup> However, also attempts have been made to access the extend of plastic deformation under sharp indenters on the basis of theories for spherical indenters.<sup>25</sup>

It is very important to note that calibration of the area function for conical indenters should always be based on the elastic modulus not the hardness since a rounded tip can shift the onset of yield to higher loads and thus lead to errors in calibrations based on hardness values.

Using the equations given above the ratio of  $HM/H$  can be estimated as:

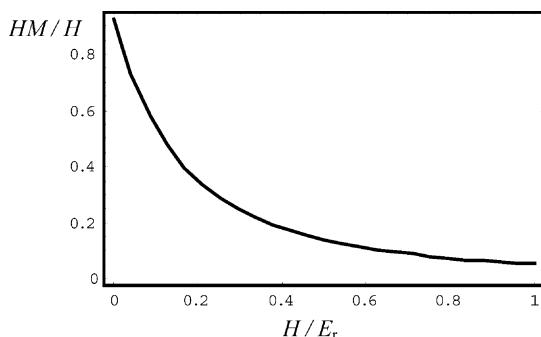


Fig. 2. The ratio  $HM$  to  $H$  as a function of the  $H/E_r$ .

$$\frac{HM}{H} = \left[ \sqrt{\frac{\alpha}{\pi(\tan \gamma)^2}} + \frac{\varepsilon}{\beta} \sqrt{\frac{\alpha \pi H}{4 E_r}} \right]^{-2} \quad (17)$$

For sphere indenters the relationship depends on the load and is rather complex and therefore not given here. The ratio of  $HM$  to  $H$  gives an indication of the effect of plastic deformation. Simple mathematical transformation of Eq. (17) will yield relationships for the dependency of  $H$  on  $HM$  and  $E_r$  or  $E_r$  on  $H$  and  $HM$ . For conical indenters the ratio  $HM$  to  $H$  as a function of the  $H/E_r$  is plotted in Fig. 2, where it can be seen that  $HM$  differs from  $H$  by approximately 10% at  $H/E_r = 0.005$ . It can be stated that the use of  $HM$  as a parameter to assess plastic deformation is only reasonably for  $H < E_r$ .

Another way to assess the plastic deformation is the use of the energy dissipated during the indentation. The elastic and plastic energies are based on the integral of the loading and unloading curve (see Fig. 3). The total work  $W_t$  can be determined via integration of Eq. (4) in combination with Eq. (14), which leads to a simple relationship for conical indenters:

$$W_t = Ph/3 = \alpha h^3 HM/3 \quad (18)$$

Thus  $HM$  is a direct measure of the total energy dissipated per indentation volume. For spherical indenters there is no simple relationship to  $HM$ , i.e. slight modification of Eq. (42) from ref. 21 leads to:

$$\begin{aligned} W_t &= \frac{\varepsilon P \sqrt{HP\pi}}{6\beta E_r} + \frac{P^2}{4HR\pi} \\ &= 2\pi HMRh \frac{1 + \frac{\sqrt{2}\pi \varepsilon H}{3 \beta E_r} \sqrt{\frac{H R}{HM h}}}{2 + \sqrt{2}\pi \frac{\varepsilon H}{\beta E_r} \sqrt{\frac{H R}{HM h}}} \end{aligned} \quad (19)$$

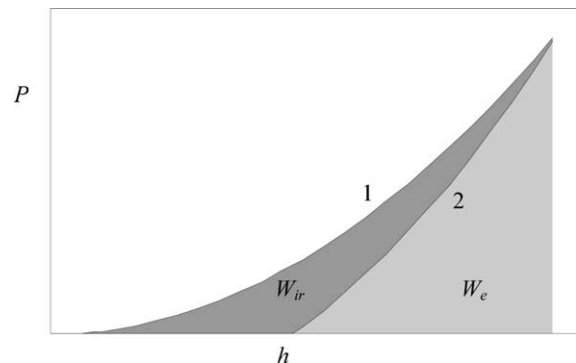


Fig. 3. Definition of the elastic energy (gray area between curve 2 and axis) and the irreversible energy (dark gray area between curves 1 and 2).

For conical indenters Cheng et al.<sup>26,27</sup> have shown graphs relating the irreversible  $W_{ir}$  to total work  $W_t$  and the ratio of  $h_f$  to  $h$  and thus the ratio of the residual depth  $H$  to  $E_r$  derived on the basis of scaling relationships in combination with finite element simulations. The underlying relationship was independent of the strain-hardening exponent and thus not influenced by pile-up or sink-in. Experimental data for monolithic materials agreed with their proposition.<sup>28</sup> Malzbender et al.<sup>29</sup> suggested that the relationship can be described by a simple linear equation and verified this experimentally for coated materials.<sup>29</sup> Recently Cheng et al. used the same description and obtained for a conical indenter with a half-angle of  $70.3^\circ$ :<sup>27</sup>

$$\frac{W_{ir}}{W_t} = 1 - \frac{W_e}{W_t} = \frac{h_f}{h} = 1 - 5.33 \frac{H}{E_r} \quad (20)$$

where  $W_e$  is the elastic energy. Venkatesh et al.<sup>30</sup> suggested on the basis of FEM simulation a factor of 5 for a Vickers indenter and 4.678 for a Berkovich indenter. Note that the contact areas under the Vickers, Berkovich and conical indenter with a half-angle of  $70.3^\circ$  have the same contact area at a particular load. Note also that, results by Bilodeau<sup>31</sup> suggest slight differences between the contact area of a Vickers, Berkovich and the equivalent cone. Another relationship has recently been suggested by Dao et al.,<sup>32</sup> however due to its complexity the relationship is not given explicitly here. Based on elastic behavior during unloading Malzbender et al.<sup>21</sup> recently derived the relationship:

$$\frac{W_{ir}}{W_t} = 1 - \frac{W_e}{W_t} = \frac{h_f}{h} = 1 - \left( \frac{\varepsilon}{2} + \frac{\beta}{\pi \tan \gamma} \frac{E_r}{H} \right)^{-1} \quad (21)$$

Eqs. (20) and (21) are compared to the results by Doa et al.<sup>32</sup> in Fig. 4. Eqs. (20) and (21) are similar up to approximately  $H/E_r \approx 0.17$  suggesting that this is the range where the unloading curve can be considered to be elastic. It can be seen easily that Eqs. (20) and (21) lead to negative values for  $W_{ir}/W_t$  at  $H/E_r \approx 0.2$  and  $\approx 0.18$ ,

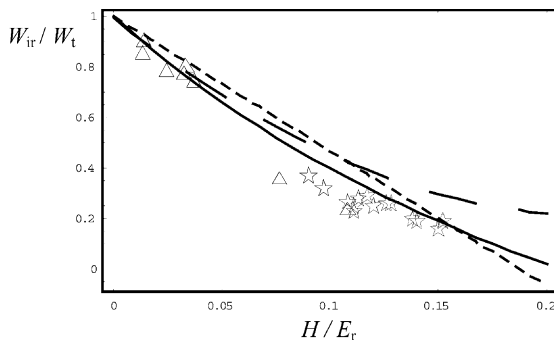


Fig. 4.  $W_{ir}/W_t$  as a function of  $H/E_r$ . Functional relationship by Malzbender et al.<sup>21</sup> (—), Dao et al.<sup>32</sup> (---), Cheng et al.<sup>27</sup> (-.-); ☆, data by Musil et al.<sup>25</sup> △, data obtained by the author.

respectively. The results of Eqs. (20) and (21) strongly diverge from the relationship suggested by Dao et al.<sup>32</sup> at  $H/E_r > 0.1$ , however, it should be remarked that Dao et al. determined their relationship by fitting data determined via FEM in a range up to  $H/E_r$  of up to approximately 0.1.

Thus, it is necessary to compare the relationships to experimental data at  $H/E_r > 0.1$  which have been recently provided by Musil et al.<sup>25</sup> Furthermore, data for  $H/E_r$  as a function of  $W_{ir}/W_t$  obtained for various materials by the author are also shown (pyrocarbon  $W_{ir}/W_t$ : 0.23, yttria stabilized zirconia—YSZ: 0.35, NiCoCrAlY 0.74, Steel-1.4742: 0.77, 8YSZ-NiO: 0.78, LaSrMn: 0.80, LaSrMn-YSZ: 0.85, 8YSZ-Ni: 0.90).<sup>33</sup> These data shown in Fig. 4 are closest to the relationship provided by Malzbender et al.<sup>21</sup> This relationship thus permits a determination of the hardness based on the ratio of the energies independent of pile-up or sink-in effects if the elastic modulus is measured using a separate technique, i.e. ultrasonic methods. A method based on the energies and the ratio of the loading to unloading slope of the load-displacement curve has been suggested previously.<sup>21</sup>

Based on Eqs. (17) and (21) a relationship for  $H$  based on the ratio of the dissipated energies can be derived, yielding:

$$\begin{aligned} H &= HM \frac{\alpha(\tan \gamma)^2}{\pi} \left[ 1 + \frac{\varepsilon}{2W_e/W - \varepsilon} \right]^2 \\ &= \frac{W_t}{h^3} \frac{3(\tan \gamma)^2}{\pi} \left[ 1 + \frac{\varepsilon}{2W_e/W - \varepsilon} \right]^2 \end{aligned} \quad (22)$$

and for the elastic modulus:

$$E_r = \frac{3}{\beta} \frac{W_e}{h^3} \left( \frac{\varepsilon W}{W_e} + \frac{2 \tan \gamma}{2 + \varepsilon W/W_e} \right) \quad (23)$$

In contrast to  $HM$  which is proportional to the total energy the indentation hardness and the elastic modulus depend on both the elastic and the total energy.

Finally, it has to be remarked that also different definitions of the elastic modulus are in use. Above we used the definition after Oliver and Pharr:<sup>3</sup>

$$E_r = \frac{dP}{dh} \sqrt{\frac{\pi}{4}} \frac{1}{\beta \sqrt{A_c}} \quad (24)$$

However, sometimes based on the use of  $h_r$  the following relationship is used:<sup>12–14</sup>

$$E'_r = \frac{dP}{dh} \sqrt{\frac{\pi}{4}} \frac{1}{\sqrt{A_r}} \quad (25)$$

resulting in the conversion formula:

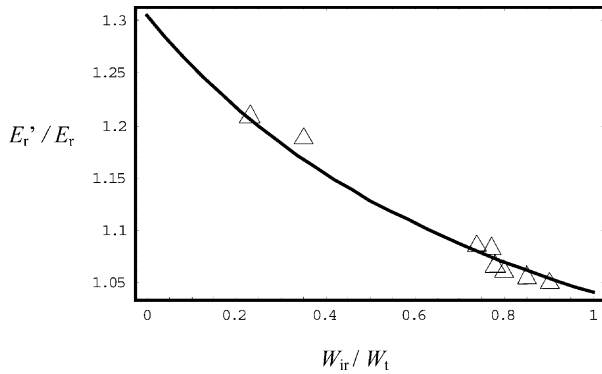


Fig. 5.  $E'_r/E_r$  as a function of  $W_{ir}/W_t$  for various materials along with a plot of Eq. (26).

$$E'_r/E_r = \beta\sqrt{A_c/A_r} = \beta\sqrt{H_{pl}/\bar{H}}$$

$$= \frac{f(n)\beta}{(1 - 1/\varepsilon) \left[ 1 + \frac{\pi \tan \gamma \varepsilon H}{2 \beta E_r} \right] + f(n)/\varepsilon} \sqrt{\frac{\pi(\tan \gamma)^2}{\alpha}}$$
(26)

Thus, the ratio of  $E'_r/E_r$  is directly related to the ratio of the dissipated energy via Eq. (21). For the assumption of no pile-up  $f(n)=1$  a plot of Eq. (26) versus  $W_{ir}/W_t$  along with data obtained by the authors and data obtained from the publication by Musil et al.<sup>25</sup> Fig. 5 shows good agreement. Thus the difference between  $E_r$  and  $E'_r$  and  $H$  and  $H_{pl}$ , respectively, can be assessed via the ratio of  $W_{ir}/W_t$ , leading to a maximum difference of 27 and 38%, respectively, at low  $W_{ir}/W_t$ , corresponding to high  $H/E_r$ .

### 3. Conclusions

The different definitions of hardness and elastic modulus are compared and relationships that permit a conversion and an assessment of the differences are derived. It has to be remarked that the dependencies are only valid for ideal indenters and imperfections such as tip rounding will result in more complex relationships. Nevertheless these relationships are useful to explain differences observed between results obtained using different analysis procedures. Special consideration is given to the relationship between the hardness under load (universal hardness) and the elastic and plastic parameters as well as to the relationship of hardness and elastic modulus to the dissipated energies.

The effects of microcracking and pore compactions that are commonly observed for ceramic materials are not treated in detail as such, however, these processes will not influence the relationships between the macroscopic variables discussed in the text as long as the procedures to determine the hardness and elastic modulus are applicable.

### Acknowledgements

The project was financially supported by the European Community within the project “Component Reliability in Solid Oxide Fuel Cell Systems for Commercial Operation (CORE-SOFC)”. Furthermore, the authors would like to thank Dr. R.W. Steinbrech and Prof. L. Singheiser for the stimulating support of the work.

### References

- Pharr, G. M. and Oliver, W. C., *MRS Bulletin*, 1992, **7**, 28.
- Wilde, H. R. and Wehrstedt, A., *Materialprüfung*, 2001, **42**, 468.
- Oliver, W. C. and Pharr, G. M., *J. Mater. Res.*, 1992, **7**, 1564.
- Chen, X. and Vlassak, J. J., *J. Mater. Res.*, 2001, **16**, 2974.
- Malzbender, J., de With, G. and den Toonder, J. M. J., *Thin Solid Films*, 2000, **372**, 134.
- Fleck, N. A., Otoyoy, H. and Needleman, A., *Int. J. Solids Structures*, 1992, **29**, 1613.
- Giannakopoulos, A. E., *Thin Solid Films*, 1998, **332**, 172.
- Nakamura, T., Quina, G. and Berndt, C. C., *J. Am. Cer. Soc.*, 2000, **83**, 578.
- Ullner, C., Germak, A., Le Doussal, H., Morrell, R., Reich, T. and Vandermeulen, W., *J. Eur. Ceram. Soc.*, 2001, **21**, 439.
- Ullner, C., Beckmann, J. and Morrell, R., *J. Eur. Ceram. Soc.*, 2002, **22**, 1183.
- Bulychev, S. I., *Tech. Phys.*, 1998, **44**, 775.
- Schwadewald, I., Bergmann, W. and Dengel, D., *Materialprüfung*, 2001, **43**, 172.
- Behncke, H. H., *Härterei-Technische Mitteilungen*, 1993, **48**, 3.
- DIN 50359.
- Ivlev, D. D., Ishlinskii, A. Y. and Nepershin, R. I., *Doklady Physics*, 2002, **47**, 630.
- Hamilton, G. M., *Proc. Inst. Mech. Eng.*, 1983, **197C**, 53.
- Sakai, M., *J. Mater. Res.*, 2002, **17**, 2161.
- Matthaei-Schulz, E. and Veters, H., *Materialprüfung*, 1999, **41**, 144.
- Heermant, C. and Dengel, D., *Materialprüfung*, 1996, **38**, 374.
- Friedrich, C., Berg, G., Broszeit, E. and Berger, C., *Thin Solid Films*, 1996, **290–291**, 216.
- Malzbender, J. and de With, G., *J. Mater. Res.*, 2002, **17**, 502.
- Andrews, E. W., Giannakopoulos, A. E., Plisson, E., Suresh, S. and Int, J., *Solids Structures*, 2002, **39**, 281.
- Hay, J. C., Bolshakov, A. and Pharr, G. M., *J. Mater. Res.*, 1999, **14**, 2296.
- Johnson, K. L., *Contact Mechanics*. Cambridge University Press, Cambridge, 1985.
- Musil, J., Kunc, F., Zeman, H. and Polakova, H., *Surf. Coat. Technol.*, 2002, **154**, 304.
- Cheng, Y.-T. and Cheng, C.-M., *Appl. Phys. Lett.*, 1998, **73**, 614.
- Y.-T. Cheng, Z. Li, C.-M. Cheng, Fundamentals of nanoindentation and nanotribology II. In *MRS Proceeding*, Vol. 694, 2001, Q1.1.
- Larsson, P.-L., *In. J. Mech. Sci.*, 2001, **43**, 895.
- Malzbender, J. and de With, G., *Surf. Coat. Technol*, 2000, **135**, 60.
- Venkatesh, T. A., van Vleit, K. J., Giannakopoulos, A. E. and Suresh, S., *Scripta Mater.*, 2000, **42**, 833.
- Bilodeau, G. G., *J. Appli. Mech.*, 1992, **59**, 519.
- Dao, M., Chollacoop, N., van Vliet, K. J., Venkatesh, T. A. and Suresh, S., *Acta Mater.*, 2001, **49**, 3899.
- Tietz, F., *Ionics*, 1999, **5**, 130.